Indian Journal of Marine Sciences
Vol. 33(1), March 2004, pp. 11-29

Satellite observations of the regional aerosol distribution and transport over the Arabian Sea, Bay of Bengal and Indian Ocean

*K Rajeev, Sandhya K Nair, K Parameswaran, & C Suresh Raju

Space Physics Laboratory, Vikram Sarabhai Space Centre, Thiruvananthapuram 695 022, India
*[E-mail: k_rajeev@vsnl.com]

Received 28 August 2003

The aerosol optical depth (AOD) derived from the NOAA14-AVHRR data and the tropospheric circulation obtained from the NCEP-NCAR reanalysis were used to study the regional distribution and long-range transport of aerosols over the oceanic areas around the Indian subcontinent during the Asian dry period (November – April) and the southwest monsoon season (June-September). Due to the contrasting airmass types, the aerosol properties over the oceanic areas around the Indian subcontinent are distinctly different during the Asian dry period compared to that during the summer monsoon season. Strikingly, the oceanic areas around the Indian subcontinent in the northern hemisphere in general, and the Arabian Sea in particular are always under the influence of continental aerosols throughout the year, despite the large annual migration of ITCZ and the presence of the vast oceanic areas at the south of the continental areas. The study demonstrates the transport of aerosols from the continental areas in the northern hemisphere to the oceanic region during the Asian dry season and a much larger-scale aerosol transport from the Arabian desert region to the Arabian Sea during the summer monsoon period. Bay of Bengal and the tropical Indian Ocean are significantly influenced by the aerosol transport from the Indian subcontinent and southeast Asia. However, the continental aerosol transport remains more or less confined to the Arabian Sea, Bay of Bengal and northern hemisphere Indian Ocean. Throughout the year, spatial gradient in AOD is large over Arabian Sea and Bay of Bengal, particularly in the meridional direction across ~5°N to 10°N. Associated with the El Nino related forest fires in the Indonesian region, a substantially large aerosol plume, with AOD exceeding 1.0, was observed over the tropical Indian Ocean during September-November 1997. The contribution of natural aerosols to the observed AOD during each season, the long-term changes in the aerosol loading, and the interaction between aerosols and clouds further needs to be investigated.

[**Key words**: Aerosols, regional aerosol distribution, transport, satellite observations, AVHRR, Indian Ocean, Arabian Sea, Bay of Bengal, forest fires]
[**IPC Code:** Int. Cl.[7] C09K 3/30, G01B 11/22]

1. Introduction

Role of atmospheric aerosols on the radiation budget of the earth-atmosphere system, the cloud microphysical properties, the hydrological cycle and the climate is well recognized[1,2]. The transport of aerosols from the source region is mainly determined by the aerosol residence time and the magnitude and direction of the prevailing winds. Due to their short atmospheric residence time (less than ~10 days), the tropospheric aerosols are distributed regionally and their abundance decreases away from the source region. Satellites provide the most suitable platform to study the regional/global distribution of aerosols and the top-of-atmosphere aerosol radiative forcing, due to their large spatial coverage[3-7]. However, the inversion of satellite-measured radiances to derive the aerosol optical depth and aerosol size distribution generally involves several assumptions, such as the reflectance of the earth's surface, the aerosol scattering and absorption properties, the altitude distribution of aerosols, and the mean state of the gaseous composition of the atmosphere. Several sensitivity analyses were carriedout to quantify the uncertainties arising from these assumptions in the derivation of aerosol optical depth (AOD) from satellite data[8-10].

The Indian Ocean region and the northern hemispheric continental areas at its north (between 40°E-100°E and 25°S-30°N) are unique in several ways. The most important of them is that the annual migration of the Inter Tropical Convergence Zone (ITCZ) is largest over this part of the globe and this migration extends from ~15°S in February to ~25°N or more in July. Further, the most intense tropical convective zone (the largest ascending limb of Walker circulation) is located at the western border of the tropical Indian Ocean. Climate zones in this region extend from deserts in the western parts to semi-arid regions in the northern parts, tropical rainforests in the southern continental areas, and the pristine oceanic

*Phone: 0471-2562330 Fax: 0471-2706535

areas in the southern hemisphere. During Asian dry season (November to April period), a large-scale high pressure system develops over the continental landmasses in this region, driving lower tropospheric northerly (northeasterly or northwesterly) winds from the continental areas towards the ITCZ (which is located at ~10°S to 15°S during this season in the western Indian Ocean)[11]. The southerly wind in the upper troposphere from the ITCZ region to the continental areas completes the Hardly circulation cell. During the Asian southwest summer monsoon period (June to September), the ITCZ migrates to north due to the intense low pressure generated in the northwestern parts of the region, and brings the massive southwest monsoon over to the Indian subcontinent. The horizontal pressure gradient and the lower tropospheric wind speeds are significantly larger during the summer monsoon period than that during the Asian dry period. However, due to the absence of efficient aerosol removal mechanisms (mainly washout and rainout), the aerosol residence time in the northern hemisphere is expected to be large during the Asian dry season compared to summer monsoon period (when the Indian subcontinent receives large rainfall). Thus during both the seasons, the aerosols can be transported to thousands of kilometers away from their source regions.

Extensive measurements of the physical, chemical and radiative properties of aerosols, their altitude and horizontal distributions, and the direct and indirect aerosol radiative forcing over the oceanic areas around the Indian subcontinent during the Asian dry period were carriedout during the Indian Ocean Experiment (INDOEX)[11] based on a variety of platforms including land, ship, aircraft, and satellite-based observations[9,12-18] [see also the special issues of J. Geophys. Res, vol.106, 2001 and Current Science (supplement), vol. 80, 2001]. However, such comprehensive measurements of the aerosols, particularly on the chemical composition of aerosols and its radiative impact, during the summer are yet to be made, though multi-year observations on aerosol properties at some of the typical continental and island locations in India and around do exist[16,19-25]. Spaceborne measurements of the regional distribution of aerosols over the continental and oceanic areas in this region were also carriedout using different satellite sensors such as AVHRR[4,9], POLDER[7], TOMS[6], MODIS[5], SeaWiFS[3], MISR[26], and IRS-P4-OCM[27]. Of these, AOD determination using the AVHRR, SeaWiFS, and OCM are limited to the oceanic areas.

Satellite observations of the regional aerosol distribution and transport during the southwest monsoon season (June-September) and the Asian dry season (November-April), over the oceanic areas around the Indian subcontinent from 25°S to 25°N and 40°E to 100°E, during 1996-1999 are presented in this paper. The aerosol distribution is derived from NOAA14-AVHRR data and the information on the tropospheric circulation is obtained from NCEP/NCAR reanalysis. Main objective of this paper is to provide a comparison between the aerosol regional distribution and transport over the Indian Ocean region during these two contrasting seasons. It should be stated here that we depend on the published results based on AVHRR-derived AOD during the Asian dry season[9,28-32].

2. Data and Method of Analysis

The aerosol optical depth (at the wavelength 630 nm ± 50 nm) over the oceanic regions around the Indian subcontinent (in the latitude range 25°S to 25°N and the longitude range 40°E-100°E) is retrieved from the radiance measured in Channel 1 of NOAA14-AVHRR. The methodology is explained elsewhere[9,29]. We have used the NOAA-14 AVHRR global area coverage (GAC) data of the afternoon satellite passes. Revised post-launch calibration constants which correct for the degradation of AVHRR channel 1 sensor are used to convert the AVHRR digital counts to reflectance[33]. Retrieval of AOD is based on comparison of the observed satellite radiance at channel 1 with the look-up tables of modeled radiances. The look-up tables of satellite radiances as a function of solar zenith angle, the satellite viewing angle, relative azimuth, surface wind speed, and AOD are generated using the discrete ordinate radiative transfer method for a plane parallel atmosphere[34] with 32 layers in vertical. This method accounts for the multiple scattering by aerosols and molecules and absorption due to aerosols, water vapor and ozone. Vertical profiles of pressure, temperature, molecular density, and ozone for tropical atmosphere are based on the model by McClatchey *et al.*[35]. In order to minimize errors in the retrieval of AOD, we use the data only from the anti-solar side of satellite scan. Variations in ocean reflectance due to wind speed are taken into account by considering daily surface winds from the NCEP/NCAR Reanalysis[36]. Fresnel reflection of the direct and diffuse solar radiation at the ocean surface is calculated for rough ocean based on the model proposed by

Cox & Munk[37]. Increase in ocean albedo due to foam (white caps) with increase in wind speed is calculated based on the model produced by Kopke[38]. Identification of the clear sky pixels is based on the threshold, channel ratio and spatial coherence methods[39,40].

Inversion of AVHRR data to derive AOD requires apriori information about the aerosol scattering phase function and single scattering albedo. Extensive observations of the scattering and absorbing properties of aerosols were carriedout using *in situ* measurements over the Indian Ocean during the Asian dry season of 1998 and 1999 (as part of INDOEX). This led to the development of the model representing the aerosol properties during the Asian dry season over the Indian Ocean[13,15]. This aerosol model contains seven aerosol types, viz. sea salt, sulfate, nitrate, organics, ammonia, dust, and soot. The scattering phase function corresponding to this aerosol composition is used here in the determination of AOD from AVHRR data during the Asian dry season. The single scattering albedo at the surface is taken as 0.90 with a column integrated value of 0.87, which is in agreement with the *in situ* observations[13,15,41]. It is also interesting to note that the Angstrom exponent observed at the Indian Ocean island, Kaashidhoo, is very consistent (between 0.97 and 1.24) during November to April period[21].

During the summer monsoon period, the lack of information of the chemical properties of aerosols prevents the development of a comprehensive model. However, it is interesting to note that several satellite based observations have demonstrated that the aerosol distribution over the Arabian Sea and Indian Ocean are significantly influenced by the transport of dust aerosols from the Arabian desert[4,8]. The 2-channel inversion of Mishchenko *et al.*[8] showed that the Angstrom exponent is very nearly uniform over the Arabian Sea, Bay of Bengal and the tropical Indian Ocean and has a mean value of ~0.4 during the summer monsoon period. This value of 0.4 is grossly in agreement with the Angstrom exponent observed at Bahrain[21,42], the Indian Ocean island of Kaashidhoo[21] and the shipborne observations at the Arabian Sea[43] during summer monsoon season. Kaufman *et al.*[44] showed that the dust aerosols are less absorbing and has a mean single scattering albedo of 0.97 in the visible region. While the contribution of dust to the observed AOD may be very high during this season, the importance of other species such as sea salt, sulfate and soot in this region cannot be neglected[45]. Dubovik *et al.*[42] reported aerosol single scattering albedo between 0.92 and 0.95 in the visible region over Bahrain (which is close to the source region of Arabian dust) during the Asian summer monsoon period. The dust laden air from the Saharan region is also found to have aerosol single scattering albedo around 0.93. The model presented by Takamura *et al.*[45] suggest aerosol single scattering albedo of ~0.9 to 0.95 over this region during summer monsoon period. Considering the above observations and models, in the present study, we assume that the aerosol size distribution is represented by modified power law[8] (MPL) with an Angstrom exponent of 0.4 and a single scattering albedo of 0.93 during the summer monsoon season.

The satellite retrieved AOD during the Asian dry season is compared with the *in situ* measured AOD[9] (as shown in figure 1 of Rajeev & Ramanathan[9]). The slope of the intercomparison between the AVHRR-derived AOD and the *in situ* values during the Asian dry period is 0.977 and intercept is 0.020. The correlation coefficient is 0.921. The RMS deviation between the AVHRR and the *in situ* AOD is 0.055. A comparison of the monthly mean *in situ* measured AOD values at Kaashidhoo (KCO)[46] during the June-September period of 1998 and 1999 with that of the AVHRR-derived AOD obtained from the present analysis (within 2 degrees around KCO) is shown in Table 1, which indicates that the AVHRR-derived and the *in situ* measured AOD values are in agreement within 0.03, except in one case when the difference is 0.07. The temporal variations observed in the *in situ*

Table 1—Intercomparison between the *in situ* measured monthly mean AOD at Kaashidhoo Climate Observatory[46] with the AVHRR derived monthly mean AOD within 2 degrees around KCO during the June-September period of 1998 and 1999.

Month & Year	Monthly mean AVHRR-AOD (630nm) within 2 degree around KCO	Standard Error AVHR R-AOD	*In situ* measured monthly mean AOD (630 nm) at KCO[46]
June 1998	0.14	0.03	0.12
July 1998	0.25	0.04	—
August 1998	0.13	0.01	0.12
September 1998	0.10	0.02	0.07
June 1999	0.16	0.02	0.13
July 1999	0.21	0.03	0.19
August 1999	0.20	0.02	0.13
September 1999	0.13	0.01	0.11

measured AOD are clearly seen in the AVHRR-derived AOD as well. However, it should be stated that the number of cloud-free days in the eastern Arabian Sea, when the satellite observation of AOD is possible, is limited (typically ~5 days per month) during the southwest summer monsoon period. Further, the days of observation used for estimating the monthly mean AOD at KCO[46] might be different from those used for estimating the monthly mean AOD from AVHRR data. Even with these limitations, the agreement between monthly mean values of AOD derived from AVHRR and those from *in situ* measurements at KCO is generally within 0.03 (except in August 1999 when the deviation is 0.07). Consideration of these, along with the fact that the monthly variation in AOD observed at KCO is well reproduced in the AVHRR-derived AOD, shows the reliability of the AVHRR-derived AOD.

The satellite derived AOD is sensitive to the aerosol phase function, the single scattering albedo, the surface reflectance and the AVHRR calibration constants used in the retrieval. The sensitivity of the above parameters on the satellite derived AOD were carriedout and are presented elsewhere[9,29]. Based on the sensitivity analysis and the intercomparison of AVHRR AOD with the *in situ* measured AOD, the typical uncertainty of the AVHRR derived AOD is approximately 15% during the Asian dry season. Considering the non-availability of *in situ* measured chemical and radiative properties of aerosols, the maximum uncertainty in AVHRR-derived AOD during summer monsoon season is expected to be slightly larger but less than 20%, with a minimum uncertainty of ~0.03.

3. Regional aerosol distribution and transport during the Asian dry season (November-April)

3.1. General characteristics of the tropospheric circulation and cloud occurrence

During November to April period, the ITCZ is generally located in the southern hemisphere (seasonal mean location between equator and ~15°S), and the continental and oceanic areas in the Asian region (particularly at south of about 30°N) experience dry weather[31]. The driest regions are Arabia and northern and central parts of Indian subcontinent, where the outgoing longwave radiation (OLR) is greater than ~290 W m^{-2} and precipitable water content less than 20 kg m^{-2}. The areal extent of this dry area increases from November (when it is limited to Arabia and the northwest India) to April (when it covers the region between 5°N and 30°N in the Arabian Sea sector and between ~10°N and 30°N in the Indian subcontinent)[31]. This feature is mainly because of the anticyclonic circulation in the lower troposphere prevailing over Arabia and the Indian subcontinent, and the increase in its areal extent from November to March[31]. The dry regions in the northern hemisphere and the ITCZ are well manifested in the frequency of occurrence of clouds. Figure 1 shows the frequency of occurrence of clouds (all cloud types; expressed in percentage) in this region during February 1998 obtained from NOAA14-AVHRR data. Figure 1 clearly shows the location of ITCZ (the intense cloud band observed at about 5°S-20°S) and its north-south tilt (location of ITCZ is at about 15°S-20°S in the western Indian Ocean while it is at about 0-5°S near the Indonesian region). The intense dry region in the northern hemisphere is clearly observed in Fig. 1, with minimum cloudiness (frequency of occurrence <10%) around 15°N. The dry region in the northern hemisphere and the intense convection in the ITCZ between equator and ~15°S are observed throughout the period of November to April. However, the location of ITCZ shows north-south migration (mainly between about 0-5°N in November to 10°S-20°S in February-March) and the absolute magnitude of fractional cloudiness varies by about 20%. Further, the areal extent of the relatively cloud free region in the northern hemisphere increases from November till around February-March and the fractional cloudiness is ~10-20% larger in April. The dryness in the northern hemisphere increases the aerosol residence time due to the absence of efficient aerosol removal mechanisms. Rasch *et al.*[47] reported the relatively larger residence time (~10 days) of atmospheric aerosols over this region during the Asian dry period.

The prevailing atmospheric circulation in the lower troposphere during February, April, and November 1998 at 850 mb are shown in Fig.2. General characteristics of the lower tropospheric circulation such as the prevailing northerly (northeasterly/northwesterly) winds, the anti-cyclonic circulation in the northern hemisphere, the ITCZ and the anticyclonic circulation in the southern hemisphere are prevailing throughout the lower troposphere (below ~4 km). These features are similar during the dry season of other years also, except for some differences during the El Nino period. The anticyclonic circulation over Arabia, and the extended anticyclonic circulation over the Indian

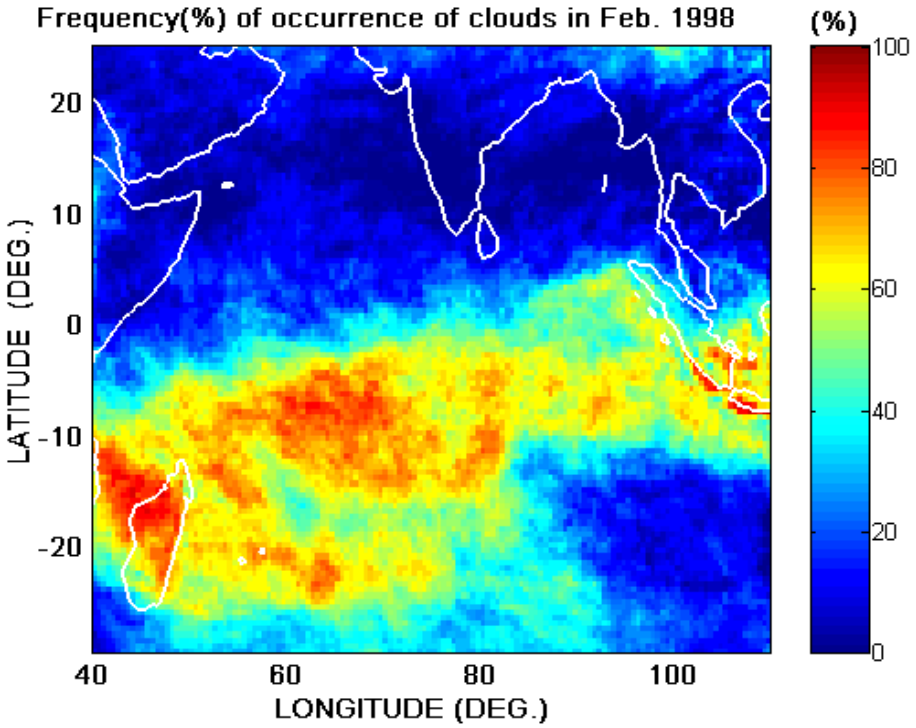

Fig. 1—Monthly mean frequency of occurrence of clouds (all clouds) during February 1998 observed using NOAA14-AVHRR data.

subcontinent are the main features of the northern hemispheric circulation at 850 mb. A northerly wind from the continental land areas prevails over the Arabian Sea. Over the Bay of Bengal, the flow is from the Indian subcontinent at north of ~5°N. South of ~5°N, easterly flow from Southeast Asia generally prevails. Over the southern hemisphere, the main features of the atmospheric circulation at 850 mb are the ITCZ along around 5°S-15°S, and an extended high pressure region at south of about 25°S. The anticyclonic circulation centered around 15°N (Fig. 2) is clearly associated with the very low frequency of occurrence of clouds (Fig. 1).

Ramanathan *et al.*[15] have shown that the aerosol loading over the Indian Ocean and Arabian Sea regions during the dry period is mostly confined to the lower troposphere (below ~4km). During the dry period the lower tropospheric northerly winds enable transport of air from the dry Asian continent in the northern hemisphere into the oceanic regions[15,29,31,48]. This airmass from the northern hemisphere and the pristine air from the southern hemisphere are connected at the ITCZ through a cross equatorial flow into the ITCZ. The monsoonal flow from north to south brings dry continental air over the ocean causing a low level temperature inversion leading to mostly clear skies with scattered cumuli and minimal rain[15].

3.2. Aerosol distribution over Arabian Sea, Bay of Bengal, and Indian Ocean

Nair *et al.*[31] have shown that the AOD in the Arabian Sea and Bay of Bengal are generally low and steady during November-January period and increases from February to April. The regional distribution of mean AOD during November-January and February-April periods of 1996-97, 1997-98, and 1998-99 over the Arabian Sea, Bay of Bengal and Indian Ocean are shown in Fig. 3. Only clear sky pixels that are not adjacent to cloudy pixels are used for estimation of AOD. The frequency of occurrence of clouds in the Arabian Sea and Bay of Bengal is very small during the dry season (<30%) and hence the frequency of occurrence of cloud-free pixels from which the AOD can be determined are generally more than 70%. At south of about 20°S, frequency of occurrence of cloud-free pixels is more than ~ 50%. However, the large cloudiness in the ITCZ region limits the frequency of occurrence of cloud free pixels to between 10 and 30%. This aspect is also explained in Rajeev & Ramanathan[9].

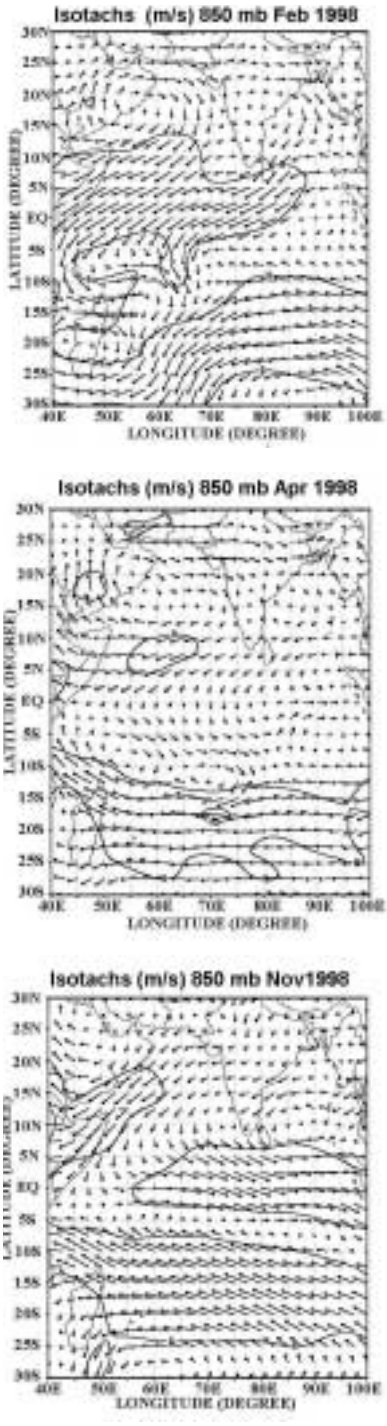

Fig. 2—Monthly mean wind vectors at 850 mb during February, April, and November 1998.

The overall geographical patterns of the aerosol distribution, particularly the north-south gradient in AOD and the locations of high AOD values, were more or less similar in all these years[9,31]. High AOD values are observed in the northern hemisphere compared to those in the southern hemisphere. Other major features observed are:

(1) Relatively high AOD values (>0.2) were encountered near the northern hemispheric continents in all the three years. Highest values of AOD over the Arabian Sea were observed near the west coast of India and coastal Arabia. Over the Bay of Bengal, the highest values of AOD were observed near the east coast of India. These features are more discernible during February-April period. An aerosol plume over Bay of Bengal off the Southeast Asia was also present during most of the observation period.

(2) In all the three years, the AOD values over the Arabian Sea and Bay of Bengal during February-April period is larger than that during the November-January period. The area encompassed by AOD > 0.2 and the average value of AOD within these high AOD pockets increases from November to April. This build-up is largest near the coastal regions of the Indian subcontinent.

(3) The highest AOD values (> 0.3) were found over the north Bay of Bengal close to the east coast of India. Perpendicular to the east coast of India, the AOD decreases rapidly with increasing distance from the coast. Similar features were observed near the coasts of southeast Asia. A central area of Bay of Bengal has relatively low AOD values (< 0.2).

(4) South of equator, AOD was generally less than about 0.15. This is significantly lower than that in the north. The ITCZ was characterised by a minimum in AOD (AOD < 0.1 between equator and ~10°S). Over the southern hemisphere Indian Ocean, south of ~10°S, the aerosol loading generally increases and AOD values often exceeds 0.1, particularly between 15°S and 20°S. The highest aerosol loading in the southern hemisphere Indian Ocean is generally observed in the western and eastern parts.

(5) A pocket of high AOD is generally observed near the northwest coast of Madagascar during November-January period (particularly during 1996-97 and 1998-99).

(6) In the northern hemisphere, AOD values show significant interannual variations, particularly during the February-April period. Highest AOD values were observed during the February-April

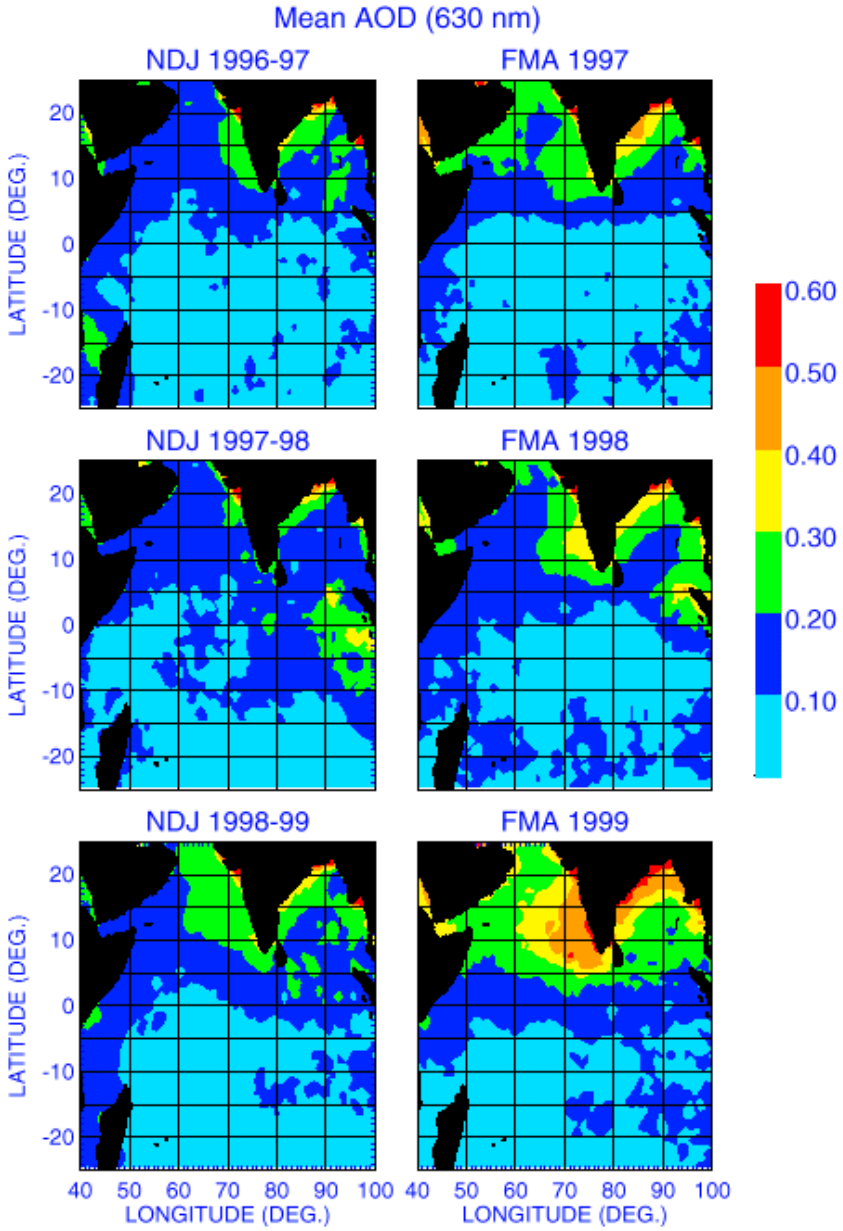

Fig. 3—Regional maps of the mean AOD (at the wavelength of 630±50 nm) during November-January (NDJ - left panel) and February-April (FMA-right panel) periods of 1996-97, 1997-98 and 1998-99 over the Arabian Sea, Bay of Bengal, and Indian Ocean.

period of 1999. The increase in AOD during 1999 is most distinctly seen near the east and west coasts of India. During the February-April period of 1999, AOD over the Arabian Sea and Bay of Bengal close to the Indian coast is higher by a factor of ~1.5 compared to that in the corresponding period of 1997 and 1998. This is consistent with the observations made on INDOEX cruises[41,49]. The AOD values near the Southeast Asia and Arabia are also higher during the dry period of 1999, though the magnitude of the increase is less.

(7) An intense aerosol plume was observed over the equatorial Indian Ocean off the Indonesian region during 1997-98. This aerosol plume has originated from the intense forest fires at Indonesia[32,50].

Figure 4 shows the latitude variations of mean AOD during November –January and February-April periods in the Arabian Sea sector (50°E-80°E) and the Bay of

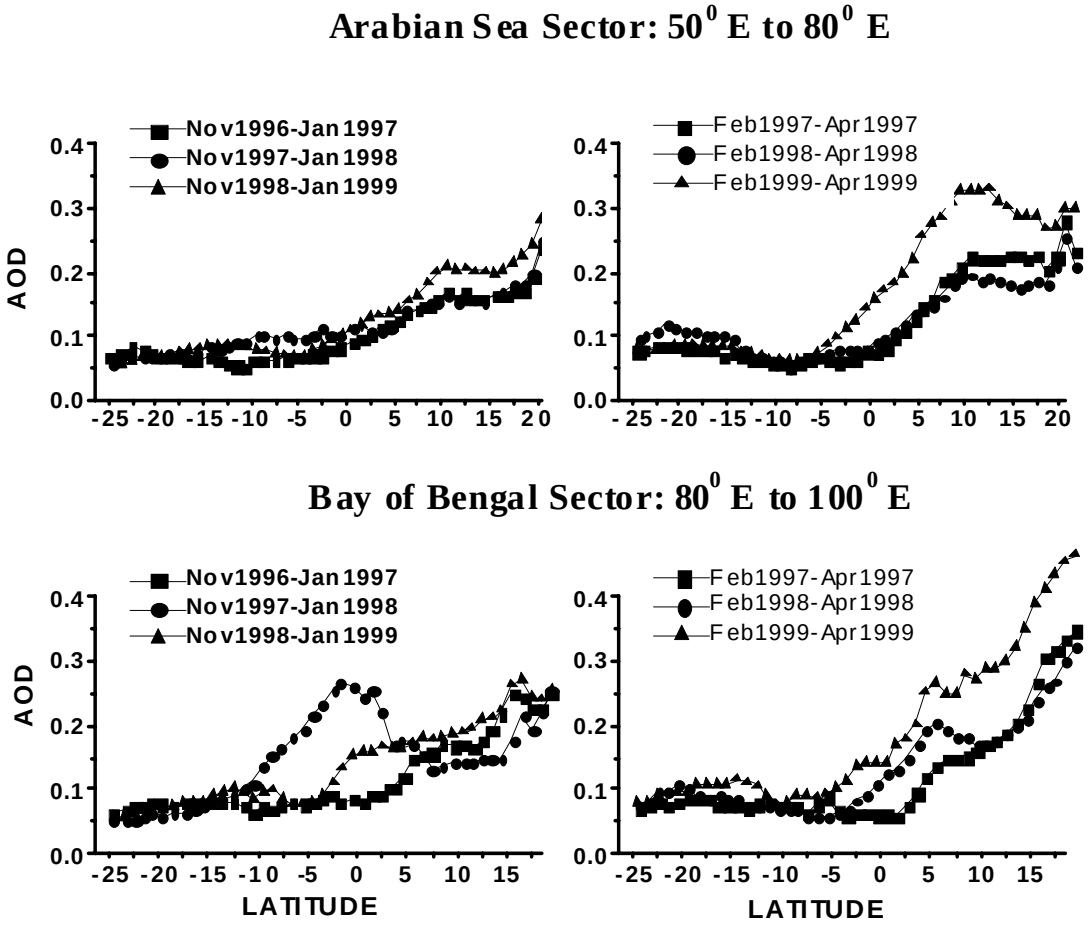

Fig. 4—Latitude variations of mean AOD during November – January (left panels) and February-April (right panels) periods in the Arabian Sea sector (between 50°E-80°E) and Bay of Bengal Sector (between 80°E-100°E).

Bengal sector (80°E-100°E). The overall latitude variations in AOD at both these longitude sectors are similar. The highest AOD was observed at the latitude region north of ~10°N. The largest latitude gradient in AOD was observed between the equator and ~10°N. This gradient is maximum during the February-April period, which can mainly be attributed to the increase in AOD in the Northern Hemisphere from February to April, while the minimum AOD observed at ~5°S remained fairly constant. The latitudinal gradient in AOD shows significant interannual variability with largest values being encountered in 1999. A small increase in AOD was observed towards the south of 10°S to reach a Southern Hemisphere peak value of ~0.1 at about 20°S. Over the Southern Hemisphere, the month-to-month and interannual variabilities in the latitude variation in AOD are negligible.

3.3. Effect of tropospheric circulation on the regional aerosol distribution.

Large scale dryness prevailing in the northern hemisphere during the November – April period increases the residence time of aerosols. This enables them to get transported to distances far away from the continental source regions through the prevailing lower tropospheric winds. The areal extent of such aerosol plumes and their geographical structure depend on the prevailing wind speed and direction. This can be seen by comparing the regional distribution of AOD shown in Fig. 3 and the lower tropospheric circulation shown in Fig. 2. The westerly winds from the Arabian continent over to the Arabian Sea during November – April period causes advection of Arabian airmass over to the northern parts of Arabian Sea[29]. This could be the main reason for the relatively high AOD observed over the coastal Arabia and

Gulf regions. Highest AOD values were observed over the Arabian Sea close to the west coast of India where the prevailing wind is northeasterly in the lower troposphere, blowing from the Indian subcontinent. Over the northwest Bay of Bengal, high AOD values were associated with the offshore flow in the lower troposphere from the Indian subcontinent. As the transport of airmass from the Indian subcontinent in November is very much limited to the coastal region, the areal extent of the aerosol plume over the Bay of Bengal is small and mostly confined to near-coast regions of the peninsular India. The aerosol plume over the southeast Bay of Bengal is linked to the easterly transport of air from Southeast Asia.

The aerosol residence time over the northern hemisphere near the Indian subcontinent was found to be about 7 to 10 days[15,47], which is higher than the globally averaged residence time of tropospheric aerosols. Dryness and its areal extent over the Indian subcontinent and Arabia increased from November to March. This might be the main reason for the increase in residence time of aerosols. The resulting increase in the aerosol accumulation can be one of the main reasons for the observed increase in AOD over the Arabian Sea and Bay of Bengal near the Indian subcontinent from November to April. Temperature and dryness over the peninsular India also generally increases from February to April. Also, the north-south aligned lower tropospheric trough over the central parts of the tropical peninsular India (along ~78°E between about 7°N and 15°N), which develops and intensifies from February to April has the potential to carry the soil dust vertically up from the dry and semi-arid regions of peninsular India. Once they reach ~850 to 700 mb levels, these aerosols can be transported over to the Arabian Sea and Indian Ocean regions through the prevailing easterlies at these levels. This also may have a contribution to the increased aerosol loading from February to April over the Arabian Sea. This aspect, however, needs to be further examined based on *in situ* observations and modeling studies.

The aerosol-rich northern hemispheric air meets with the pristine air from the southern hemisphere at the ITCZ. The ITCZ is characterised by large-scale convection, cloudiness and rainfall. The increased rainfall leads to effective removal of aerosols through washout and rainout which might be the prime cause for the low values of the AOD observed at the ITCZ. The Southern Hemisphere Indian Ocean is generally free from major aerosol sources and hence the month-to-month and interannual variations are insignificant. South of ITCZ, the lower tropospheric winds are predominantly easterly. Wind speed is highest between 15°S to 25°S. The high surface winds leading to the generation of sea salt aerosols might be one of the main reasons for the increased aerosol loading observed in this region. Over the Horn of Africa, near the equatorial Indian Ocean, the wind has a significant northerly component and this air sometimes crosses the equator to reach north of Madagascar, as observed in Fig. 3. The spatial distribution of aerosols over the equatorial Indian Ocean, south of the Horn of Africa, seen in Fig. 3 indicates a cross equatorial flow and interhemispheric transport of aerosols during the Asian dry period.

During February-April period of 1999, aerosol loading over the Arabian Sea and Bay of Bengal was higher than that during the corresponding periods of the previous years by a factor of ~1.5. It is important to note that (1) the increase in AOD observed during February-April period of 1999 is significantly larger than that observed from November 1998 to January 1999, (2) the increase in AOD is very large over the eastern regions of the Arabian Sea and western regions of the Bay of Bengal which are near the Indian Subcontinent, and (3) an elevated aerosol layer at around 2 to 3 km region was observed by aircraft and lidar measurements during the Intensive Field Phase of the INDOEX (January to March 1999)[14,15]. Nair *et al.*[31] investigated the probable reasons for the increased aerosol optical depth observed during the later half of the dry season of 1999 and suggested that the increased aerosol loading observed might be due to a combination of the following features: (1) the northward position of the extended anti-cyclonic circulation over the Indian subcontinent during 1999 (by about 3 degrees compared to 1997 and 1998), (2) stronger easterly flow prevailing over the Indian subcontinent south of about 18°N in 1999 which brings larger airmass from the continental areas over to the oceanic regions, and (3) nearly continuous ITCZ in the 40°E-100°E longitude region during 1999 compared to weaker and broken ITCZ during other periods, and (4) northward position of ITCZ during 1999 (by about 3 degrees) compared to 1997 and 1998.

4. Forest fires in Southeast Asia and the aerosol distribution over the Indian Ocean

Generally, forest fires occur over the southeast Asia (particularly Indonesian region) during August-

November period[50]. Due to large-scale dryness, the forest fires intensify during El Nino years, producing massive amounts of carbonaceous (mainly organic) aerosols[32,50]. Further, during El Nino periods, the lower and mid-tropospheric winds over the tropical Indian Ocean are predominantly easterly aiding westward transport of smoke generated from the forest fires in Southeast Asia. The El Nino event of 1997-1998 followed by the La Nina in 1998-1999 was the strongest of its kind encountered in the 20th century[51]. Associated with this event Indonesia experienced severe drought leading to large-scale forest fires. Large aerosol plumes from these fires advected over the equatorial Indian Ocean region.

Parameswaran *et al.*[32] studied the development and decay of this plume and its regional transport using the aerosol optical depth derived from the NOAA14-AVHRR data along with the tropospheric circulation and meteorological conditions derived from NCEP/NCAR reanalysis. The aerosol optical depth were derived using the smoke model developed by integrating the observations of chemical, physical and optical properties of smoke aerosols arising from of forest fires in the tropical region[52] with the properties of aerosols described by Hess *et al.*[53]. This smoke aerosol model is composed of organics (60%), black carbon (5%), sea salt (20%) and sulfate (15%)[32] [values in the bracket indicate the percentage of each species by mass]. The aerosol single scattering albedo for the smoke model is 0.9 which is same as the value of the aerosol single scattering albedo observed by Nakajima *et al.*[50] during the Indonesian forest fire events in 1997. The AVHRR derived AOD was compared with the *in situ* measured AOD at Singapore[50], and the slope of the regression line[39] between the two observations is 1.06.

Figure 5 shows the mean AOD observed during September-November period of 1997 when the intense forest fires occurred over the Indonesian region. Significantly high AOD values (AOD > 0.5) were observed over equatorial Indian Ocean during this period. In the first half of September, the plume was confined to the coastal regions of Indonesia which started extending towards west over the equatorial Indian Ocean to reach up to 60°E by October**.** The spatial extent of this aerosol plume increased from the first half of September[32]. The AOD in the plume region is highest in the second half of October which covered the longitude extent from ~110°E to ~60°E in the equatorial region. The aerosol plume is mainly confined to the equatorial region and the prevailing horizontal transport in this region is along the zonal direction. This results in the large meridional gradient in AOD. Decay of the plume started by the first half of November and the AOD in this geographical region resumed its normal value (< 0.2) by the first half of December 1997.

The winds in the troposphere up to about 200 mb over the eastern equatorial Indian Ocean were predominantly easterly during the period of September-

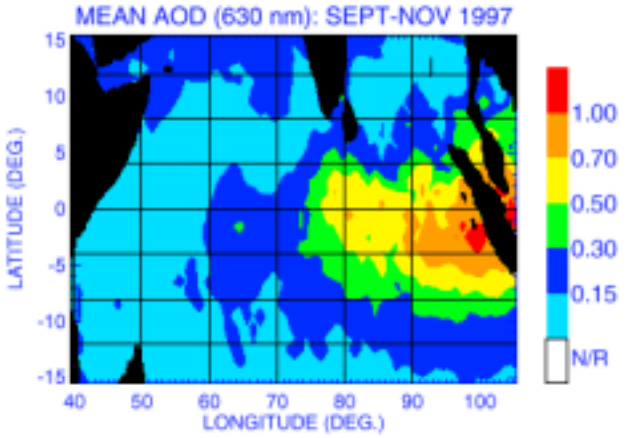

Fig. 5—Regional map of the mean AOD during September-November period of 1997 over the tropical Indian Ocean. (N/R indicates the locations where AOD could not be retrieved due to the presence of clouds).

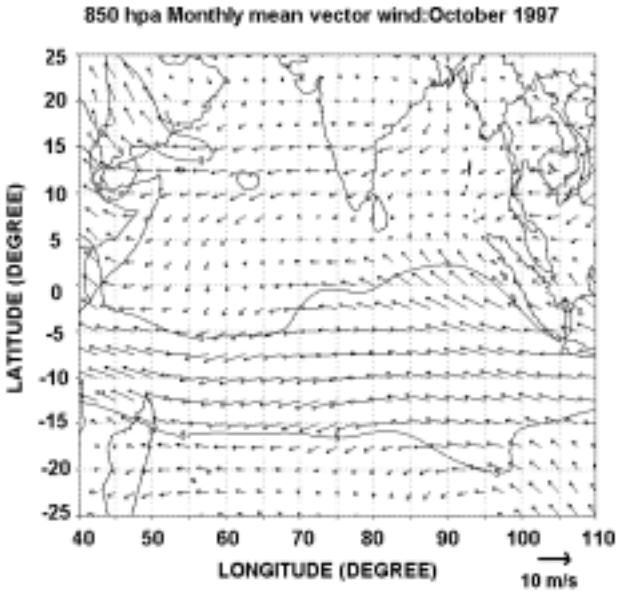

Fig. 6—Monthly mean winds at the 850 mb level during October 1997 obtained from NCEP-NCAR reanalysis. The contours of the wind speeds are marked at intervals of 5 ms^{-1}.

November 1997 under the influence of El Nino, as compared to the predominantly westerly winds over this region during the normal years. Figure 6 shows the wind vectors at 850 mb level during October 1997, which shows predominantly easterly winds in the eastern Indian Ocean, in comparison with the wind vectors shown in Fig.2 during November 1998 (which represents the wind pattern during a normal year). This easterly wind at the equatorial Indian Ocean is responsible for the transport of aerosols originated from the Indonesian forest fires over to the tropical Indian Ocean. Another important feature during the El Nino period of 1997 is the large-scale convergence over the western equatorial Indian Ocean between 50°E and 60°E during the September-November period of 1997. Associated with this, large cloudiness and rainfall occurred at the western equatorial Indian Ocean, as revealed from the NCEP-NCAR reanalysis. This might have prevented the spreading of this smoke plume further westward of about 60°E, particularly during October 1997. A close association was observed between the aerosol optical depth over equatorial Indian Ocean and the fire counts over Southeast Asia derived from Along Track Scanning Radiometer data[32].

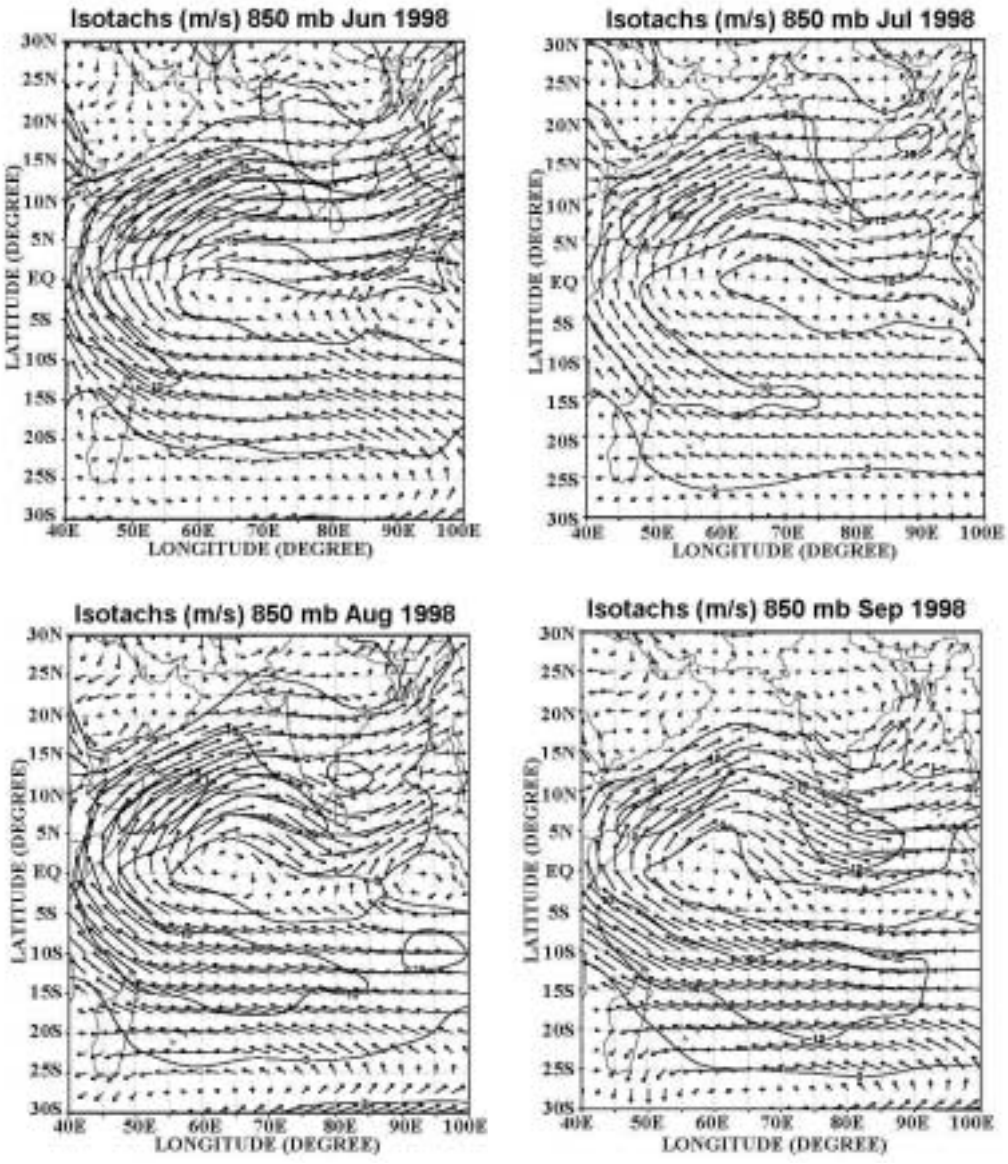

Fig. 7—The monthly mean wind vectors during June, July, August and September 1998 at 850 mb level.

5. Regional aerosol distribution during the summer monsoon season (June-September)

5.1. General characteristics of the tropospheric circulation and cloud occurrence

During June to September, the high north-south pressure gradient produces large-scale cross equatorial flow from the southern hemisphere to the northern hemisphere through the lower troposphere leading to the southwest Asian summer monsoon. Over the Arabian Sea and the peninsular India (south of the monsoon trough), the monsoon circulation has a strong westerly component. The prevailing atmospheric circulation at 850 mb during June-September 1998 is shown in Fig. 7, and the main features observed are:

(1) Northward transport of oceanic airmass from the southern hemisphere over to the continental areas in the northern hemisphere, with largest cross-equatorial flow at the western Indian Ocean (west of 50°E, with wind speed exceeding ~15 m s^{-1}). Another area of significantly large cross-equatorial flow is along 80°E-90°E longitude region (wind speed ~5-10 m s^{-1}).

(2) Wind speed in the southern hemisphere is largest around 10°S-20°S (wind speed of about10 m s^{-1}, which is largely easterly).

(3) Over the Arabian Sea, the wind speed is generally more than ~10 m s^{-1}, and has a strong westerly component (southwesterly in the western parts and northwesterly in the eastern parts). High wind speeds are observed at the western Arabian Sea, close to Somalia, particularly in the geographical region between 5°N - 15°N and 50°E - 60°E (Somalia jet). The Somalia jet wind speed increases from ~15 m s^{-1} in June to more than 20 m s^{-1} in July, and decreases subsequently to ~15 m s^{-1} in August and ~10 m s^{-1} in September.

(4) Over the Bay of Bengal, the wind is generally southwesterly, with wind speed more than ~10 m s^{-1} in June and ~5 – 10 m s^{-1} in July, August, and September.

(5) The wind over the Indian peninsular region (particularly at the south of ~20°N) is generally westerly, with wind speeds ~5 to ~10 m s^{-1}. Over the Indian peninsular region, the wind speed is generally less than that observed over the oceanic areas around it.

(6) Except in the coastal regions and the Horn of Africa, the wind over the West Asian continental land mass (mainly desert region) is very weak, but generally northwesterly. Over the coastal region of Arabia, the wind is ~2 - 5 m s^{-1}, and is mainly westerly. The airmass from the West Asian desert areas (though the wind speeds are less) get mixed with the strong westerly winds observed over the Arabian Sea, throughout the monsoon period.

Figure 8 shows the frequency of occurrence of clouds (all clouds; expressed in percentage) over the region during July 1998. The pattern is somewhat similar during June-September, except that the cloudiness over the Indian region and the adjoining Arabian Sea and Bay of Bengal differs by ~10–20 % depending on the location and month. The west Asian region and the coastal regions of west Arabian Sea were cloud free (frequency of occurrence of clouds generally less than ~20%). The frequency of occurrence of clouds was largest in the central and eastern Arabian Sea (70-100%) compared to western Arabian Sea (10–60%). The frequency of occurrence of clouds over Bay of Bengal and the equatorial Indian Ocean is 60-100% and that at the southern hemisphere Indian Ocean south of ~15°S was less than 30%. In most of the areas over the Arabian Sea and Bay of Bengal, frequency of cloud occurrence was high in July and August, compared to June and September. Even though the large amount of rainfall encountered in this season significantly reduces the aerosol residence time, the strong prevailing winds observed might enable the long range transport of aerosols.

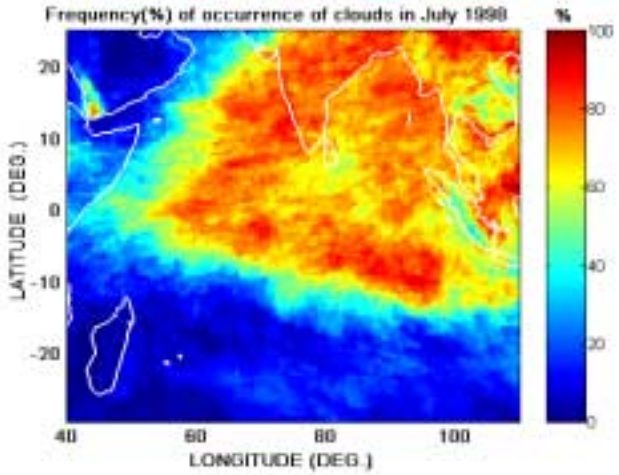

Fig. 8—Frequency of occurrence of clouds (all clouds, in percentage) observed during July 1998 using NOAA14-AVHRR data.

5.2 Regional aerosol distribution during the southwest monsoon season

At the western Arabian Sea and the south Indian Ocean, the number of clear sky AVHRR pixels was high (50-80% of the pixels are cloud free in these regions). Due to the large cloudiness, the number of AVHRR pixels that can be used for retrieving AOD is low over eastern Arabian Sea, Bay of Bengal and equatorial Indian Ocean (0-30% of the pixels). The seasonal mean regional aerosol distribution during the summer monsoon season (June-September) of 1997, 1998, and 1999 are shown in Fig. 9. The main features observed are:

(1) Over the whole of Arabian Sea, very large AOD was observed throughout the summer monsoon period. The AOD is largest in the western parts of Arabian Sea. On an average, AOD over the Arabian Sea is highest during the summer monsoon period compared to rest of the year.

(2) Over the Arabian Sea, the magnitude of AOD and the area covered by AOD exceeding 0.3 increases from June to reach its maximum in July, followed by a decrease through August and September.

(3) The spatial variation in the seasonal mean AOD was significantly high, with maximum variation observed in the meridional direction around 15°N in the Arabian Sea.

(4) The AOD over Bay of Bengal was smaller than that over Arabian Sea, though it was more than 0.2 over the western parts of Bay of Bengal.

(5) The seasonal mean AOD was generally less than 0.2 over the equatorial Indian Ocean (mainly between about 5°N and 5°S). However, over the western parts of the equatorial Indian Ocean, AOD often exceeded 0.1. (The high AOD values observed at the eastern equatorial Indian Ocean during 1997 was associated with the forest fire event described in the previous section).

(6) Over the southern hemisphere Indian Ocean (SHIO) between about 10°S and 20°S, the AOD exceeded 0.1.

(7) The regional distribution of AOD showed significant interannual variability over the Arabian Sea. However, the magnitude of the interannual variability during the summer monsoon season was less that that observed during the February-April period. The AOD during 1999 was larger by ~0.1 compared to that during 1997 and 1998.

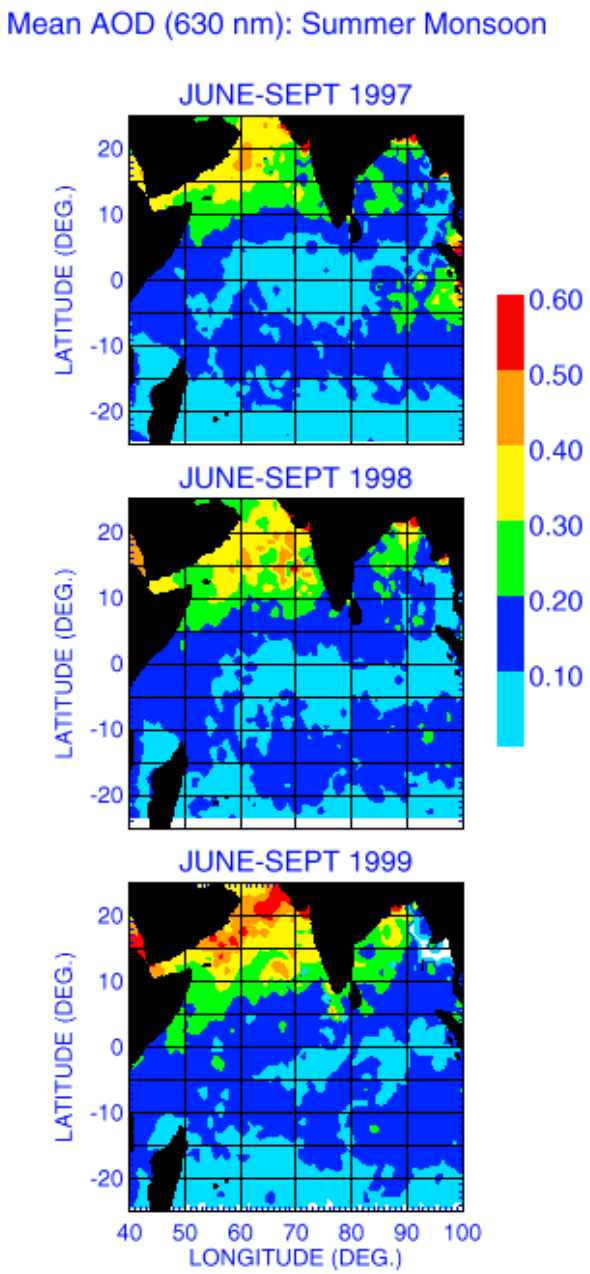

Fig. 9—Mean AOD during the southwest summer monsoon season (June-September) of 1997, 1998, and 1999.

The interannual variability over Bay of Bengal was lesser than that over the Arabian Sea, and was negligible in the SHIO.

Figure 10 shows the latitude variation in AOD (averaged in the longitude region between 50°E and 80°E; Arabian Sea sector) during the summer monsoon season of 1997, 1998 and 1999. Latitude variation in AOD is strikingly similar during all the three

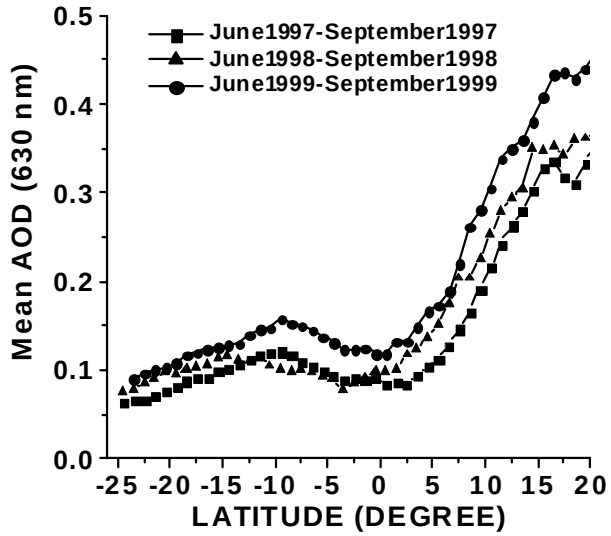

Fig. 10—Latitude variation of the mean AOD during the southwest summer monsoon season (June – September) of 1997, 1998, and 1999 over the Arabian Sea (50°E-80°E).

years, though the absolute values of AODs are different. North of equator, the AOD value increases steadily with increase in latitude (almost a monotonic increase) upto ~15°N. This is in contrast to the behavior observed during the dry season when the latitude variation is high between the equator and ~10°N, and the AOD remained somewhat similar between ~10°N and ~15°N. The latitude variation in AOD in the summer monsoon season was maximum between 5°N and 15°N, and is higher than that observed in the dry season. Minimum AOD (AOD<0.1) was observed at near the equator. South of the equator, AOD increased up to ~10°S to 15°S (where the regional mean AOD is in the range of 0.10 to 0.16). These observations are consistent with the results obtained by Li & Ramanathan[46].

5.3. Effect of transport on the regional aerosol distribution during summer monsoon.

A comparison between the prevailing atmospheric circulation shown in Fig. 7 and the regional distribution of aerosols shown in Fig. 9 clearly reveals the effect of aerosol transport from the West Asian desert region over to the oceanic areas around the Indian subcontinent (mainly over the Arabian Sea). Though the wind speeds over the continental areas of the west Asia are generally small (as seen from Fig. 7), the wind direction is predominantly northwesterly over the northwestern regions. This might be responsible for bringing large amount of mineral dust from the desert regions. Once these dust particles reach the coastal regions of Arabia and Horn of Africa, they are very quickly transported eastward by the strong westerlies prevailing over the coastal Arabia and the adjoining oceanic regions. For example, the wind speed (mainly westerly) observed during the southwest monsoon season over the Arabian Sea at 850 mb is typically in the range of 10 m s^{-1} to 20 m s^{-1}, which corresponds to an eastward transport of about 850 to 1700 km per day (The dust aerosols over the Arabian Sea during southwest monsoon period were also observed by TOMS justifying the above hypothesis). Assuming that the aerosols are not lost due to washout or rainout, the travel time from the western border of Arabian Sea to the west coast of India will be about 2 to 4 days. Note that that westerly wind speed increase from June to July over the west Arabian Sea (particularly over Somalia). Associated with this, the absolute value of the AOD over the Arabian Sea as well as the area covered by the large aerosol plume increases from June to July. The westerly wind speeds decrease in August leading to an overall decrease in AOD over the Arabian Sea. The westerly winds over the west Arabian Sea further weaken during September, which is clearly associated with further decrease in AOD observed over the Arabian Sea.

High AODs observed over the west Bay of Bengal also might be contributed by the dust transport, but needs to be confirmed. However, AOD over Bay of Bengal is significantly less during the summer monsoon period compared to that over Arabian Sea. It may also be noted that the rainfall over the eastern parts of Arabian Sea and the whole of Bay of Bengal is very large and this might lead to effective removal of the aerosols. This might be the main reason for the low AOD observed over Bay of Bengal compared to that over the Arabian Sea, though the westerly wind speeds are high over the whole region (Fig. 7).

As seen from the NCEP/NCAR reanalysis data, the surface wind speed (1000 mb level) is high over the Arabian Sea and Bay of Bengal during the summer monsoon period. The overall wind pattern is similar to that observed at 850 mb, but the wind speeds are less by about 0 - 5ms^{-1} at the regions of high wind speeds. Larger surface wind speeds also can lead to increase in AOD through increase in the production of sea salt aerosols. Based on the empirical relation given by Erickson *et al.*[54]. [AOD(U)=AOD(U=0)*exp(0.16U), where U is the wind speed in ms^{-1}, and AOD(U=0) is

the AOD at zero wind speed], and assuming that the AOD at zero wind speed is 0.02 (minimum AOD obtained in the present analysis), the sea salt contribution to AOD works out to be ~0.1 or less over most of the Arabian Sea and Bay of Bengal regions (wind speed ~10 m s^{-1} or less). At regions where the surface wind speeds are very high (e.g., off Somalia in the western Arabian Sea where the wind speed is ~15 m s^{-1}), the sea salt contribution to the observed AOD could be as high as 0.2. This might be one of the reasons for the higher AOD values observed at the high wind speed region off Somalia (particularly during July and August when the wind speed is largest). This is further supported by the higher AOD values (~0.15) observed around 10°S - 15°S, where the wind speed is larger than 10 m s^{-1}.

6. Discussion

The spatial distribution of aerosols over the Arabian Sea, Bay of Bengal and the equatorial Indian Ocean during the summer monsoon season (June-September) is distinctly different from that during the Asian dry season (November-April). The lower tropospheric winds are predominantly from the northern continental land masses into the oceanic areas at the south during the November to April period, while the wind is from the southern hemisphere to northern hemisphere during the summer monsoon period. The summer monsoon circulation system has a strong westerly wind component over the Arabian Sea and Bay of Bengal, resulting in the very large transport of dust particles from the Arabian desert regions during this season into the Arabian Sea. Similar observations were also made in the earlier studies[4,22,43,46,55]. The AOD in the Arabian Sea is largest during the summer monsoon season compared to the other seasons. As is shown in the present study, large westerly wind speeds observed during this period enables the efficient transport of mineral dust from the Arabian region over to the west coast of India (travel time of 2-4 days) where the lower tropospheric wind is northwesterly. Over and above, most of the central and eastern Arabian Sea and Bay of Bengal are cloudy and rainy during the summer monsoon season. This could reduce the aerosol residence time in the atmosphere and also hinder the further eastward transport of dust aerosols over to Bay of Bengal. These meteorological phenomena could lead to the confinement of Arabian dust mainly to Arabian Sea, as observed. Large cloudiness suppresses the aerosol direct radiative forcing (assuming that the aerosols are mainly residing below the cloud top level). But the influence of high AOD observed in the less-cloudy west Arabian Sea (and presumably over the desert regions of West Asia where we do not have data) on the regional climate, atmospheric circulation, and dynamics of the southwest monsoon needs to be studied based on models[56,57]. The month to month variation in AOD over Bahrain[21,42] (close to the Arabian desert regions) is very consistent with the month to month variations observed over the Arabian Sea in the present study. At Bahrain, minimum AOD values are observed during November to March (AOD at 500 nm is in the range of 0.21 to 0.24) and the AOD increases from April (AOD ~ 0.33) up to July (AOD ~0.48), and decreases thereafter[21]. At Kaashidhoo, though the absolute value of AOD is smaller during summer monsoon season (compared to the February – April period), the maximum AOD during the summer monsoon is observed to be higher during July[21,46], and is consistent with the present observations [see Table 1] as well as the AOD observed at Bahrain[21,42]. Over the Arabian Sea, AOD shows a steady increase with latitude from ~5°N to 15°N. The aerosol radiative forcing resulting from this can modulate the meteorological parameters and influence the atmospheric circulation system. This brings out the importance of monitoring the change in aerosol loading at these regions for investigating its impact on regional climate.

In contrast to the summer monsoon season, the cloudiness and rainfall over the study area is significantly less during the November-April period (the Asian dry season). The regional mean AOD is minimum over the Arabian Sea and Bay of Bengal during the November-January period. During the second half of the Asian dry season (February-April), both over the Arabian Sea and Bay of Bengal, the AOD values are larger than that during the first half (November-January). This increase in AOD from February to April is not uniform over all the areas. It is larger near the continents, particularly near the southeast Arabian Sea and northwest Bay of Bengal. The latitude gradient in AOD between the equator and ~10°N is very large particularly during the February-April period, and it is largest over the Bay of Bengal. Large interannual variability in AOD and its spatial gradient are observed in Arabian Sea and Bay of Bengal during February-April period. The impact of this and the resulting changes in aerosol radiative forcing on the energy budget of the earth-atmosphere system needs to be investigated. Angstrom parameter during the Asian dry period is

higher compared to that during the summer monsoon period, showing the dominance of smaller size particles during the November - April period[21]. However, the fraction of natural to anthropogenic aerosols is yet to be quantified. Origin and sustenance of a significantly large aerosol layer observed around 2-4 km altitude region over the Indian Ocean is to be understood[14]. The mean AOD (column atmosphere) as well as the aerosol extinction coefficient in the boundary layer also shows an increasing trend over some of the continental locations during the past one decade[58]. These variations might have long-term effect on the climate[59].

The aerosols released into the atmosphere due to the forest fires in the Indonesian region produces significant impact on the regional distribution of aerosols over the tropical Indian Ocean during strong El Nino events when the tropospheric circulation in this region is easterly. We report here the regional aerosol distribution and transport during the 1997 El Nino period, when an intense aerosol plume (AOD exceeding 1.0) had extended from the Indonesian region up to ~60°E in the tropical Indian Ocean. The development and decay of the plume during the September to November period of 1997 and its association with fire counts were reported by Parameswaran *et al*.[32]. This is an excellent case to study the aerosol-cloud interaction (the region being somewhat cloudy, but not overcast during this period), the aerosol radiative forcing and the overall effect on the temperature and energy budget of the earth-atmosphere system. However, the variations in all these parameters arising from the changes in the El Nino activity itself[51] during the period is a major hindrance for such a study.

One of the most striking features observed over the oceanic regions around the Indian subcontinent in general and over the Arabian Sea in particular is that, these areas are under the influence of continental aerosols throughout the year, though the ITCZ migrates by more than ~35° from the oceanic areas in the southern hemisphere to the continental areas in the northern hemisphere during the course of the year. The continental aerosol transport to these oceanic areas is minimum during November-January period and maximum during June-September. The cloudiness shows large spatial variations (both in the frequency of occurrence and cloud type) at south of ~5°N during the dry season, which coincides with the region of large spatial variations in aerosol loading. On the other hand, during summer monsoon season, the cloud cover is large over the Arabian Sea region where the aerosol loading also is high (with large spatial variations in cloud occurrence near the west Arabian Sea). This provides a challenging scientific problem to observe the aerosol-cloud interaction and the total aerosol radiative forcing (including direct and indirect effect) due to different aerosol types[2,60,61] and compare with the model predictions.

Conclusion

The regional distribution and transport of aerosols during the Asian dry period and the summer monsoon season were studied using the AOD derived from NOAA14-AVHRR data and the tropospheric circulation obtained from the NCEP-NCAR reanalysis. The main conclusions are:

(1) The spatial distribution of aerosols over the Arabian Sea, Bay of Bengal and the equatorial Indian Ocean are distinctly different during the summer monsoon season (June-September) compared to the Asian dry season (November-April). The AOD over all these areas are minimum during November-January period.

(2) Over Arabian Sea and Bay of Bengal, particularly near the southeast Arabian Sea, Coastal Arabia, and northwest Bay of Bengal, the aerosol loading and its latitude variation during February-April period is larger than those during the November-January period.

(3) The AOD values as well as its latitude gradient over the Arabian Sea are maximum during the southwest summer monsoon season. This is largely governed by the transport of mineral dust from the Asian desert regions. The contribution of the sea salt generated by high surface wind speed also is significant in this season.

(4) The AOD over the southern hemisphere Indian Ocean is less than ~0.15 during most of the periods and the interannual variability is negligible.

(5) The interannual variability in AOD is large during February-April period over the Arabian Sea and Bay of Bengal. Changes in the lower tropospheric circulation play a major role in governing this interannual variability.

(6) Forest fires in Indonesia, particularly during the El Nino periods, are found to have significant influence in the aerosol distribution over the equatorial Indian Ocean.

(7) Arabian Sea and Bay of Bengal are under the influence of continental aerosols throughout the year, despite the large annual migration of ITCZ.

The distribution of aerosols and clouds over these oceanic regions which are under the influence of contrasting

arimasses (and the aerosol properties) during the dry season and the summer monsoon season provide excellent opportunities for studying the aerosol-cloud interaction and the total aerosol radiative forcing due to different types of aerosols and clouds. Deposition of aerosols to the ocean surface and the changes in the photosynthetically active radiation (PAR) due to atmospheric aerosols might be important to the marine life as well. Satellite observations of phytoplankton, regional distribution and properties of aerosols and clouds and the radiation budget of the earth-atmosphere system based on the present and future generation of Indian Satellites together with the data from other satellites can play a vital role in this study.

Acknowledgement

The NCEP/NCAR reanalysis was provided by the NOAA-CIRES Climate Diagnostics Center, Boulder Colorado (through web site at http://www.cdc.noaa.gov). The NOAA14-AVHRR raw data was obtained from the NOAA-Satellite Active Archive.

References

1 Haywood, J M, Ramaswamy V & Soden B J, Tropospheric aerosol climate forcing in clear-sky satellite observations over the oceans, *Science*, 283 (1999) 1299-1303.

2 Ramanathan, V, Crutzen P J, Kiehl J T & Rosenfeld D, Aerosols, climate and hydrological cycle, *Science*, 294 (2001) 2119-2124.

3 Gordon, H R & Wang M, Retrieval of water-leaving radiance and aerosol optical thickness over oceans with SeaWiFS: A preliminary algorithm, *Appl Opt*, 33 (1994) 443-452.

4 Husar, R B, Prospero J M & Stowe L L, Characterization of tropospheric aerosols over the ocean with the NOAA AVHRR optical thickness operational product, *J Geophys Res*, 102 (1997) 16889-16909.

5 Kaufman, Y J, Tanre D, Remer L A, Vermote E F, Chu A & Holben B N, Operational remote sensing of tropospheric aerosol over land from EOS moderate resolution imaging spectroradiometer, *J Geophys Res*, 102 (1997) 17051-17067.

6 Torres, O, Bhartia P K, Herman J R, Ahmad Z & Gleason J, Derivation of aerosol properties from satellite measurements of backscattered ultraviolet radiation: theoretical basis, *J Geophys Res*, 103 (1998) 17099-17110.

7 Goloub, P, Tanre D, Deuse J L, Herman M, Marchand A & Breon F M, Validation of the first algorithm applied for deriving the aerosol properties over the ocean using the POLDER/ADEOS measurements, *IEEE Trans Geosci Remote Sens*, 37 (1999) 1586-1596.

8 Mishchenko, M, Geogdzhayev I V, Cairns B, Rossow W B & Lacis A A, Aerosol retrievals over the ocean by use of channels 1 and 2 AVHRR data: sensitivity analysis and preliminary results, *App Opt*, 38 (1999) 7325-7341.

9 Rajeev K & Ramanathan V, Direct observations of clear-sky aerosol radiative forcing from space during the Indian Ocean Experiment, *J Geophys Res*, 106 (2001) 17, 221-17, 236.

10 Ignatov A, Sensitivity and information content of aerosol retrievals from the Advanced Very High Resolution Radiometer: radiometric factors, *App Opt*, 41 (2002) 991-1011.

11 Ramanathan, V, Crutzen P J, Coakley J, Clarke A, Collins W D, Dickerson R, Fahey D, Gardoud B, Heymensfield A, Keihl T J, Kuettner J, Krishnamurti T N, Lubin D, Maring H, Ogran J, Prospero J, Rasch P J, Savoie D, Shaw G, Tuck A, Valero F P J, Woodbridge E L & Zhang G, *Indian Ocean Experiment (INDOEX), A multi-agency proposal for field experiment in the Indian Ocean*, C4 Publ 162 (Scripps Institution of Oceanography, La Jolla, California, USA) 1996.

12 Jayaraman, A, Lubin D, Ramachandran S, Ramanathan V, Woodbridge E, Collins W D & Zalpuri K S, Direct observations of aerosol radiative forcing over the tropical Indian Ocean during the January-February 1996 pre-INDOEX cruise, *J Geophys Res*, 103 (1998) 13827-13836.

13 Satheesh, S K, Ramanathan V, Li-Jones X, Lobert J M, Podgorny I A, Prospero J M, Holben B N & Loeb N G, A model for the natural and anthropogenic aerosols over the tropical Indian Ocean derived from Indian Ocean Experiment data, *J Geophys Res*, 104 (1999) 27, 421-27, 440.

14 Ansmann, A, Althausen D, Wandinger U, Franke K, Muller D, Wagner F & Heintzenberg J, Vertical profiling of the Indian aerosol plume with six-wavelength lidar during INDOEX: a first case study, *Geophys Res Letts*, 27 (2000) 963-966.

15 Ramanathan V, Crutzen P J, Lelieveld J, Mitra A P, Althausen D, Anderson J, Andreae M O, Cantrell W, Cass G R, Chung C E, Clarke A D, Coakley J A, Collins W D, Conant W C, Dulac F, Heintzenberg J, Heymsfield A J, Holben B, Howell S, Hudson J, Jayaraman A, Kiehl J T, Krishnamurti T N, Lubin D, McFarquhar G, Novakov T, Ogren J A, Podgorny I A, Prather K, Priestley K, Prospero J M, Quinn P K, Rajeev K, Rasch P, Rupert S, Sadourny R, Satheesh S K, Shaw G E, Sheridan P, Valero F P J, Indian Ocean Experiment: An integrated analysis of the climate forcing and effects of the great Indo-Asian haze, *J Geophys Res*, 106 (2001) 28, 371-28, 398

16 Moorthy K K, Saha A, Prasad B S N, Niranjan K, Jhurry D & Pillai P S, Aerosol optical depths over peninsular India and adjoining oceans during INDOEX campaigns: spatial, temporal and spectral characteristics, *J Geophys Res*, 106 (2001), 28539-28554.

17 Kamra, A K, Murugavel P, Pawar S D & Gopalakrishnan V, Background aerosol concentration derived from the atmospheric electric conductivity measurements made over the Indian Ocean during INDOEX, *J Geophys Res*, 106 (2001) 28643-28651.

18 Ramachandran, S & Jayaraman A, Premonsoon aerosol mass loading and size distribution over Arabian Sea and the tropical Indian Ocean, *J Geophys Res*, 107 (2002) 4738, doi:10 1029/2002JD002386

19 Niranjan, K, Babu Y R, Satyanarayana G V & Thulasiraman S, Aerosol spectral optical depths and typical size distributions at a coastal urban location in India, *Tellus*, 49B (1997) 439-446

20 Satheesh S K & Moorthy K K, Aerosol characteristics over coastal regions of the Arabian Sea, *Tellus*, 49B (1997) 417-428.

21 Holben B N, Tanré D, Smirnov A, Eck T F, Slutsker I, Abuhassan, N, Newcomb W W, Schafer J S, Chatenet B,

Lavenu F, Kaufman Y J, Vande Castle J, Setzer A, Markham B, Clark D, Frouin R, Halthore R, Karneli A, O'Neill N T, Pietras C, Pinker R T, Voss & K, Zibordi G, An emerging ground based aerosol Climatology: aerosol optical depth from AERONET, *J Geophys Res*, 106(2001) 12067-12097.

22 Moorthy K K & Satheesh S K, Characteristics of aerosols over a remote island, Minicoy in the Arabian Sea: Optical properties and retrieved size characteristics, *Quart J Roy Meteorol Soc*, 126 (2000) 81-109.

23 Raju N V, Prasad B S N, Narasimhamurthy B & Thukarama M, Meteorological and anthropogenic influences on the atmospheric aerosol characteristics over a tropical station Mysore (12 degrees N), *Indian J Rad Space Phys*, 29 (2000) 115-126.

24 Devara P C S, Maheskumar R S, Raj P E, Pandithurai G & Dani K K, Recent trends in aerosol climatology and air pollution as inferred from multi-year lidar observations over a tropical urban station, *Int J Climatol*, 22 (2002) 435-49.

25 Moorthy K K, Suresh Babu S & Sathesh S K, Aerosol spectral optical depths over the Bay of Bengal: role of transport, *Geophys Res Letts*, 30 (2003) doi:10 1029/2002GL016520.

26 Diner D J, Abdou W A, Bruegge C J, Conel J E, Crean K A, Gaitley B J, Helmlinger M C, Kahn R A, Martonchik J V, Pilorz S H & Holben B N, MISR aerosol optical depth retrievals over southern Africa during the SAFARI-2000 dry season campaign, *Geophys Res Letts*, 28 (2001) 3127-3130.

27 Das I, Mohan M & Moorthy K K, Detection of marine aerosols with IRS P4-Ocean Colour Monitor, *Proc Indian Acad Sci* (*Earth Planet Sci*), 111 (2002) 425–435.

28 Rajeev K & Ramanathan V, The Indian Ocean experiment: Aerosol forcing obtained from satellite data, *Adv Space Res*, 29 (2002) 1731-1740.

29 Rajeev K, Ramanathan V & Meywerk J, Regional aerosol distribution and its long-range transport over the Indian Ocean, *J Geophys Res*, 105 (2000) 2029-2043.

30 Rajeev K, Sandhya K Nair & Parameswaran K, Seasonal and inter-annual variability of regional aerosol distribution over the Indian Ocean observed using NOAA-14 AVHRR, in *Ocean optics: Remote sensing and underwater imaging*, Edited by R J Frouin, G D Gilbert, *Proc SPIE(USA)*, 4488 (2002), 238-247.

31 Nair S K, Rajeev K & Parameswaran K, Wintertime regional aerosol distribution and the influence of continental transport over the Indian Ocean, *J Atmos Sol Terr Phys*, 65 (2003) 149-165.

32 Parameswaran K, Sandhya K Nair & K Rajeev, Impact of Indonesian forest fires during the 1997 El Nino on the aerosol distribution over the Indian ocean, *Adv Space Res* In Press (2003).

33 Rao C R N & Chen J, Revised post launch calibration of the visible and near infrared channels of the advanced very high resolution radiometer (AVHRR) on the NOAA-14 space craft, *Int J Rem Sens*, 20 (1999) 3485-3491.

34 Stamnes K, Tsay S–C, Wiscombe W & Jayaweera K, A numerically stable algorithm for discrete-ordinate-method radiative transfer in multiple scattering and emitting layered media, *App Opt*, 27 (1998) 2502-2509.

35 McClatchey R A, Fenn R W, Selby J E A, Volz F E, Garing J S, *Optical properties of the atmosphere* (third edition), Environmental Research Papers, No 411 (Air Force Cambridge Research Laboratories, Bedford, MA,USA) 1972.

36 Kalnay E, Kanamitsu M, Kistler R, Collins W, Deaven D, Gandin L, Iredell M, Saha S, White G, Woollen J, Zhu Y, Chelliah M, Ebisuzaki W, Higgins W, Janowiak J, Mo K C, Ropelewski C, Wang J, Leetmaa A, Reynolds R, Jenne R & Joseph D, The NCEP/NCAR Reanalysis 40-year Project, *Bull Amer Meteor Soc*, 77 (1996) 437-471.

37 Cox C & Munk W, Measurement of the roughness of the sea surface from photographs of the sun-glitter, *J Opt Soc Am*, 44 (1954) 838-850.

38 Koepke P, Effective reflectance of oceanic whitecaps, *Appl Opt*, 23 (1984) 1816-1824.

39 Coakley J A & Bretherton F P, Cloud cover from high-resolution scanner data: Detecting and allowing for partially filled fields of view, *J Geophys Res*, 87 (1982) 4917-4932.

40 Durkee P A, Pfeil F, Frost E & Shema R, Global analysis of aerosol particle characteristics, *Atmos Environ*, 25A (1991) 2457-2471.

41 Jayaraman A, Satheesh S K, Mitra A P & Ramanathan V, Latitude gradient in aerosol properties across the Inter Tropical Convergence Zone: Results from the joint Indo-US study onboard Sagar Kanya, *Curr Sci (Supplement*), 80(2001) 128-137.

42 Dubovik O, Holben B, Eck T F, Smirnov A, Kaufman Y J, King M D, Tanre D & Slutsker T, Variability of absorption and optical properties of key aerosol types observed in worldwide locations, *J Atmos Sci*, 59 (2002) 590-608.

43 Vinoj V & Satheesh S K, Measurements of aerosol optical depth over Arabian Sea during summer monsoon season, *Geophys Res Letts*, 30 (2003) doi:10 1029/2002GL016664.

44 Kaufman Y J, Tanre D, Dubovik O, Karnieli A & Remer L A, Absorption of sunlight by dust as inferred from satellite and ground-based remote sensing, *Geophys Res Letts*, 28 (2001) 1479-1482.

45 Takemura T, Nakajima T, Dubovik O, Holben B N & Kinne S, Single scattering albedo and radiative forcing of various aerosol species with a global three-dimensional model, *J Clim*, 15 (2002) 333-352.

46 Li F & Ramanathan V, Winter to summer monsoon variation of aerosol optical depth over the tropical Indian Ocean, *J Geophys Res*, 107 (2002), 10 1029/2001JD000949.

47 Rasch P, J, Collins W D & Eaton B E, Understanding the Indian ocean experiment (INDOEX) aerosol distribution with an aerosol assimilation, *J Geophys Res*, 106 (2001) 7337-7355.

48 Krishnamurti T N, Jha B, Prospero J, Jayaraman A & Ramanathan V, Aerosol and pollutant transport and their impact on radiative forcing over the tropical Indian Ocean during the January-February 1996 pre-INDOEX cruise, *Tellus*, 50B (1998) 521-542.

49 Parameswaran K, Nair P R, Rajan R & Balasubrahamanyam D, Spatial distribution of aerosol concentrations over the Arabian Sea and the Indian Ocean during IFP of INDOEX, *Curr Sci (Supplement)*, 80 (2001) 161-165.

50 Nakajima T, Higurashi A, Takeuchi N & Herman J R, Satellite and ground-based study of aerosol properties of 1997 Indonesian forest fire aerosols, *Geophys Res Letts*, 26 (1999) 2421-2424.

51 Asnani G C, El Nino of 1997-1998 and Indian Monsoon, *Mausam*, 52 (2001) 57-66.

52 Kreidenweis S M, Remer L A, Bruintjes R & Dubovik O Smoke aerosols from biomass burning in Mexico: Hygroscopic smoke optical model, *J Geophys Res*, 106 (201) 4831-4844.

53 Hess M, Kopke P & Schult I, Optical properties of aerosols and clouds: The software package Opac, *Bull Am Meteorol Soc*, 79 (1998) 831-844.

54 Erickson D J, Merill J T & Duce R A, Seasonal estimates of global atmospheric sea-salt distribution, *J Geophys Res*, 91 (1986) 1067-1072.

55 Prospero J M, Ginoux P, Torres O, Nicholson S E & Gill T E, Environmental characterisation of global sources of atmospheric soil dust identified with the NIMBUS 7 Total Ozone Mapping Spectrometer (TOMS) absorbing aerosol product, *Rev Geophys*, 40 (2002) doi 10 1029/2000RG000095.

56 Boucher O, Pham M & Sadourny R, General circulation model simulations of the Indian summer monsoon with increasing levels of sulphate aerosols, *Ann Geophys*, 16 (1998) 346-352.

57 Srinivasan J, A simple thermodynamic model for seasonal variation of monsoon rainfall, *Curr Sci*, 80 (2001) 73-77.

58 Parameswaran K, Rajan R, Vijayakumar G, Rajeev K, Moorthy K K, Nair P R & S K Satheesh: Seasonal and long term variations of aerosol content in the atmospheric mixing region at a tropical station on the Arabian sea coast, *J Atmos Sol Terr Phys*, 60 (1998) 17-25.

59 Krishnan R & Ramanathan V, Evidence of surface cooling from absorbing aerosols, *Geophys Res Letts*, 29 (2002) 10 1029/2002GL014687.

60 Norris J R, Has northern Indian Ocean cloud cover changed due to increasing anthropogenic aerosol, *Geophys Res Letts*, 28 (2001) 3271-3274.

61 Coakley J A & Walsh C D, Limits of aerosol indirect radiative effect derived from observations of ship tracks, *J Atmos Sci*, 59 (2002) 668-680.